IOP Publishing Journal of Physics D: Applied Physics
J. Phys. D: Appl. Phys. 49 (2016) 065305 (6pp) doi:10.1088/0022-3727/49/6/065305

Bending influence of the electrocaloric effect in a ferroelectric/paraelectric bilayer system

Y Li[1], S P Lin[1], Y J Wang[1], D C Ma[1] and Biao Wang[1,2,3]

[1] Sino French Institute of Nuclear Engineering and Technology, Sun Yat-sen University, Zhuhai 519082, People's Republic of China
[2] State Key Laboratory of Optoelectronic Materials and Technologies, Sun Yat-sen University, Guangzhou 510275, People's Republic of China
[3] School of Physics and Engineering, Sun Yat-sen University, Guangzhou 510275, People's Republic of China

E-mail: madecai@mail.sysu.edu.cn and wangbiao@mail.sysu.edu.cn

Received 5 October 2015, revised 23 November 2015
Accepted for publication 30 November 2015
Published 14 January 2016

Abstract
The influence of bending behavior on the electricaloric (EC) effect is investigated by adopting a thermodynamic model of ferroelectric (FE)/paraelectric (PE) bilayer. The polarization transitions driven by the bending effect occur at a certain temperature range, glass-like transitions, which are found to dramatically impact the EC response. A large range of EC response can be obtained from the FE/PE bilayer which is attributed to the varying misfit strain across the film thickness arising from the bending effect. The results suggest that careful choice of thickness ratio between FE and PE layers allows one to harness the intrinsic and extrinsic contributions to obtain the optimized EC response, which presents great potential for solid refrigeration application.

Keywords: ferroelectricity, electrocaloric effect, bilayer, bending effect

(Some figures may appear in colour only in the online journal)

1. Introduction

The electrocaloric (EC) effect refers to the adiabatic temperature change of materials in response to an applied external electric field [1–10]. It is a main property of ferroelectric materials which is induced by the change of entropy in the electric insulators and was first discovered in 1930 [1]. This property of ferroelectric (FE) materials has attracted increasing attention for their promising applications, like solid-state refrigeration, along with the features of environmental-friendly and high efficiency [2–5]. Nevertheless, several challenges restricting the commercial applications of the EC effect have been revealed [6–10].

When selecting a material for use as a working body in EC refrigeration, one must ensure that its EC effect, translated as entropy variation ΔS and temperature change ΔT whilst altering electric field, is large. From Maxwell's equations it follows that the EC effect may be predicted from temperature evolution of polarization induced by an electric field. To achieve high EC performances, the use of phase transitions is found to be a powerful tool since the largest EC effect usually occurs near the phase transition [11–15]. In addition, in order to tune the properties of EC materials, several methodologies, such as composition, mechanical boundary conditions, and domain structure [16–22], can be adopted to enhance the EC response. Furthermore, to meet the demand of a wide working temperature range for many devices, the strain is investigated to deal with the challenge of the narrow working temperature near the ferroelectric-paraelectric (PE) phase transition [23]. On the other hand, with the miniaturization of modern electronic devices, cooling them with a high performance becomes a problem. One possible solution is the application of low-dimensional ferroelectrics, such as ferroelectric ultrathin films and nanotubes [24–27]. The enhanced polarization-strain coupling can alter the polarization distribution, the ferroelectric transition temperature and the EC properties [28, 29].

As is well known, the physical properties of ferroelectric films grown on substrate depend largely on surface and boundary effects [30, 31]. Similarly, in recent years, it has become quite popular to investigate the EC response of bilayer films. The artificially fabricated bilayer films represent a giant room temperature electrocaloric effect depending on the relative thickness of the two layers and the film orientation. It was shown that the electrostatic coupling between the ferroelectric layer and the paraelectric layer could induce some remarkable properties [32–35]. Although extensive studies about the EC effect have been investigated to solve these challenges, the refrigeration application for some special devices such as bending chips has seldom been investigated in the literature. In this sense, a bending film/substrate system due to the same thickness order of two layers arouses our inspiration. This system was documented about a century ago [36]. The special strain gradient, strong stresses and other features of this classical model have been analyzed and applied in many fields which makes them completely different from other flat films [37–39].

In this study, in order to investigate the contribution of bending behaviors to the EC effect, the classical FE/PE bilayer system is constructed. In contrast to the traditional study, we are particularly interested in the polarizations, the derivatives of polarization with respect to temperature as well as the adiabatic temperature changes with various external electric fields. A large value of the adiabatic temperature change in a wide temperature range is found in the FE/PE bilayer. The mechanism of this wide temperature range with large adiabatic temperature change is also analyzed in detail.

2. Model and method

Here, the bilayer system is shown in figure 1(a), where h and H are the thicknesses of the layers and L is the length respectively. As for the coordinate, $z = 0$ is located at the interface of two layers, and the locations of $z = h$ and $z = -H$ present the free interfaces respectively.

To simplify the discussion, only z-direction problem along the thickness is considered and all the variables are independent of x and y such as the polarization $P_1 = P_2 = 0$ and $P_3 = P_z$. such that the total free energy of this system is given as

$$F = F_{\mathrm{Lan}} + F_{\mathrm{Grad}} + F_{\mathrm{Ela}} + F_{\mathrm{Ele}} + F_{\mathrm{Flex}} = \int_{-H}^{h} (f_{\mathrm{Lan}}(z) + f_{\mathrm{Grad}}(z) + f_{\mathrm{Ela}}(z) + f_{\mathrm{Ele}}(z) + f_{\mathrm{Flex}}(z))\mathrm{d}z \quad (1)$$

where F_{Lan} is the Landau free energy. F_{Grad} is gradient energy. F_{Ela} and F_{Ele} refer to the elastic energy and electric field energy of the bilayer system, respectively. F_{Flex} is flexoelectric coupling energy. $f_{\mathrm{Lan},}$ f_{Grad}, f_{Ela}, f_{Ele} and f_{Flex} are the corresponding energy densities.

For a perovskite ferroelectric, e.g. $BaTiO_3$, the Landau free energy density can be expressed up to a eight-order polynomial expansion at zero stress as [40]

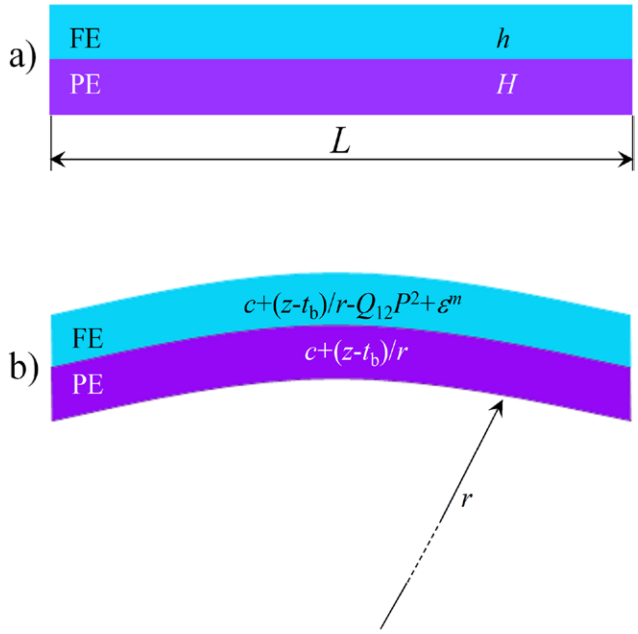

Figure 1. (a) Schematic of the FE/PE bilayer system. (b) Final bending status induced by asymmetric stress.

$$f_{\mathrm{Lan}} = \alpha_1 P^2 + \alpha_{11} P^4 + \alpha_{111} P^6 + \alpha_{1111} P^8 \quad (2)$$

where α_1, α_{11}, α_{111} and α_{1111} are the expansion coefficients of the Landau free energy.

The gradient energy, which presents the contribution of the domain walls to the total free energy, is introduced through the gradient of the polarization field. This gradient energy density f_{Grad} in bilayer can be written as

$$f_{\mathrm{grad}} = \frac{1}{2} D \left(\frac{\partial P}{\partial z} \right)^2 \quad (3)$$

with D being the gradient energy coefficients.

The elastic energy density contribution f_{Ela} can be written as

$$f_{\mathrm{Ela}} = \frac{1}{2} G_i \varepsilon_i^2 \quad (4)$$

where ε_i represent the elastic strains and i represent the PE (A) or FE (B) layer. G_A and G_B are the effective elastic constants which can be expressed by elastic stiffness of the PE and FE layers C_{11}^A, C_{12}^A; C_{11}^B, C_{12}^B respectively. So it gives that $G^A = C_{11}^A + C_{12}^A - 2(C_{12}^A)^2/C_{11}^A$ and $G^B = C_{11}^B + C_{12}^B - 2(C_{12}^B)^2/C_{11}^B$. The final bending system induced by asymmetric stress is shown in figure 1(b). According to Hsueh and Evans's bending bilayer model [33, 34, 36, 41], the total strains of PE and FE layers can be written as

$$\varepsilon_A = c + \frac{z - t_{\mathrm{b}}}{r} \qquad \text{for } -H \leqslant z \leqslant 0$$
$$\varepsilon_B = c + \frac{z - t_{\mathrm{b}}}{r} - Q_{12}P^2 + \varepsilon^{\mathrm{m}} \quad \text{for } 0 \leqslant z \leqslant h \quad (5)$$

where c is an uniform elastic strain and $z = t_{\mathrm{b}}$ is the location of the bending axis. r is the radius of curvature and Q_{12} is the electrostrictive coefficient. ε^{m} is the misfit strain between two layers which can be expressed by the lattice constants of PE and FE layers a_s, a_f and $\varepsilon^{m} = (a_s - a_f)/a_s$.

In addition, the strain distributions in the FE/PE bilayer system depend on three parameters, c, t_b and r which can be solved from three equilibrium conditions.

To start with, with the zero resultant force shown in figure 1(a) and the treatment of Hsueh and Evans [33, 34], we have

$$\int_{-H}^{0} G^{A} c\mathrm{d}z + \int_{0}^{h} G^{B}(c - Q_{12}P^{2} + \varepsilon^{m})\mathrm{d}z = 0 \tag{6}$$

Secondly, the force equilibrium in figure 1(b) gives

$$\int_{-H}^{0} G^{A}\frac{z - t_b}{r}\mathrm{d}z + \int_{0}^{h} G^{B}\frac{z - t_b}{r}\mathrm{d}z = 0 \tag{7}$$

At last, the torque equilibrium in figure 1(b) requires

$$\int_{-H}^{0} G^{A}\left(c + \frac{z - t_b}{r}\right)z\mathrm{d}z + \int_{0}^{h} G^{B}\left(c + \frac{z - t_b}{r} - Q_{12}P^{2} + \varepsilon^{m}\right)z\mathrm{d}z = 0 \tag{8}$$

According to equations (6)–(8), the uniform strain c, the position of the bending axis t_b and the radius of the curvature r can be written as functions of PE layer thickness H, FE layer thickness h and the time t [41, 42].

$$c(h, H, t) = -\frac{G_A h}{G_A H + G_B h}\left(\varepsilon^{m} - \frac{Q_{12}}{h}\int_{0}^{h} P^{2}\mathrm{d}z\right)$$
$$t_b(h, H) = \frac{G_B h^{2} - G_A H^{2}}{2(G_B h + G_A H)}$$
$$r(h, H, t) = \frac{G_A H^{2}(2H + 3t_b) + G_B h^{2}(2h - 3t_b)}{3\left(G_A c H^{2} - G_B c h^{2} - G_B \varepsilon^{m} h^{2} + 2G_B Q_{12}\int_{0}^{h} zP^{2}\mathrm{d}z\right)} \tag{9}$$

From equations (4)–(9), the elastic energy can be calculated. Then the electric field energy density f_{Ele} refers to the effect of an external electric field E_{ext}. As for the depolarization electric field E_d, it can be neglected because of the large thickness of the film and in order to concentrate on the bending behavior of the system [38, 41]. So the contribution of the f_{Ele} can be expressed as

$$f_{\mathrm{Ele}} = -E_{\mathrm{ext}}P \tag{10}$$

Finally, so as to study the effect of the coupling between polarization and strain gradients on bending system, the last term in equation (1)—the flexoelectricity needs to be taken into account. For the purpose of our model, it can be written as

$$f_{\mathrm{Flex}} = -\frac{f}{2}\left(P\frac{\partial \varepsilon_B}{\partial z} - \varepsilon_B\frac{\partial P}{\partial z}\right) \tag{11}$$

where f is the flexocoupling coefficient.

The polarization profile $P(z)$ in various applied electric fields at different temperatures can be numerically derived from the time dependent Ginzburg–Landau equation integrating with the equations (2)–(8)

$$\frac{\partial P(z, h, H, t)}{\partial t} = -M\frac{\delta F}{\delta P} \tag{12}$$

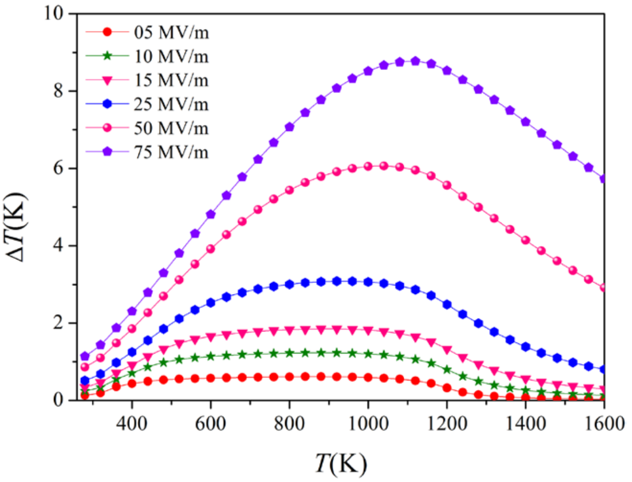

Figure 2. Adiabatic temperature changes as functions of the temperature under different electric field variations in case of $H = h = 0.1$ mm.

where M is the kinetic coefficient related to the domain wall mobility. In order to solve the equation (12), on the right hand, Euler–Lagrange equation is applied. As a result, this equation becomes a differential formula as follow:

$$\frac{\partial P}{\partial t} = -M\left(\alpha * P + \beta * P^{3} + \alpha_{111}P^{5} + \alpha_{1111}P^{7} - D\frac{\mathrm{d}^{2}P}{\mathrm{d}z^{2}} - E_{\mathrm{ext}} - f\frac{\partial \varepsilon_B}{\partial z}\right) \tag{13}$$

where $\alpha^{*} = \alpha_1(T - T_c) - 4GQ_{12}\left(c(h, H, t) + \frac{z - t_b(h, H)}{r(h, H, t)} + \varepsilon^{m}\right)$, $\beta^{*} = \alpha_{11} + 4GQ_{12}^{2}$.

At last, adiabatic temperature changes ΔT of the system under electric field variation from E_1 to E_2 are given by

$$\Delta T = -\frac{1}{C_p}\int_{E_1}^{E_2} T\left(\frac{\partial <P>}{\partial T}\right)_E \mathrm{d}E \tag{14}$$

where C_p is the heat capacity of FE layer's material. $<P>$ is the mean polarization of the FE layer

3. Results and discussions

The results are derived from the $BaTiO_3/SrTiO_3$ bilayer system where h and H represent the thickness of two layers respectively. The material constants for the Landau energy, electrostrictive coefficients, the flexocouping coefficient and the elastic properties can be found from [40, 43][4]. We fix the thickness of the FE layer $h = 0.1$ mm with the thickness step $\Delta z = 10$ nm and the lateral dimension L is $50h$.

Figure 2 shows the adiabatic temperature change of bending film as functions of temperature under different electric field variation with $h = H = 0.1$ mm. It can be seen that the value of adiabatic temperature changes gradually increase to 1.1 K at 440 K with a 15 MV m^{-1} electric field variation.

[4] $\alpha_1 = 4.124(T - 388) \times 10^{5}$ C^{-2}m^{2}N, $\alpha_{11} = -209.7 \times 10^{6}$ C^{-4}m^{6}N, $\alpha_{111} = 129.4 \times 10^{7}$ C^{-6}m^{10}N, $\alpha_{1111} = 3.863 \times 10^{10}$ C^{-8}m^{14}N, $Q_{12} = -0.034$ C^{-2}m^{4}, $C_{11}^{A} = 1.78 \times 10^{11}$ N m^{-2}, $C_{12}^{A} = 0.964 \times 10^{11}$ N m^{-2}, $C_{11}^{B} = 3.36 \times 10^{11}$ N m^{-2}, $C_{12}^{B} = 1.07 \times 10^{11}$ N m^{-2}, $a_s = 0.3905$, $a_f = 0.401$, $f = 7.8$ V.

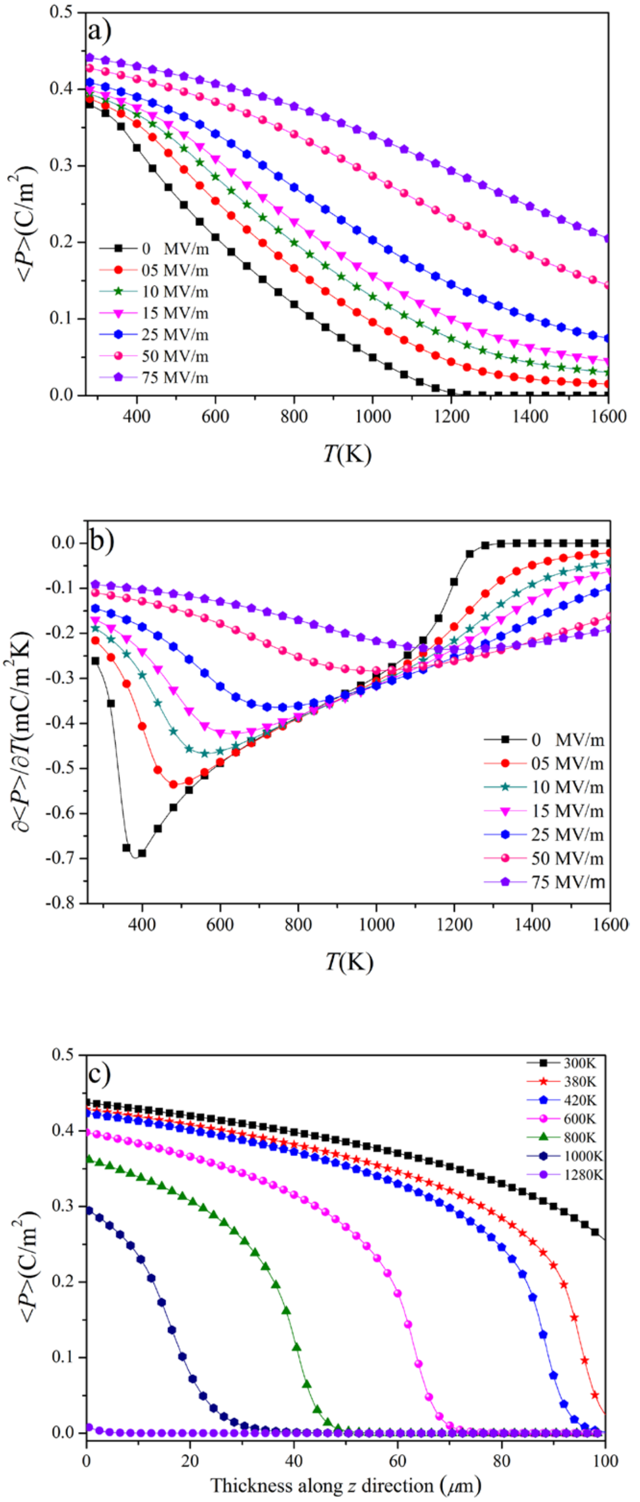

Figure 3. (a) Polarizations, (b) derivatives of polarization with respect to temperature as functions of the temperature with dynamic external electric fields and (c) distributions of polarization along z-direction at different temperature without external electric field, in case of $H = h = 0.1\,\text{mm}$.

After that, it maintains ΔT larger than 1.1 K until $T = 1075\,\text{K}$ and thus leads to a platform of adiabatic temperature change. As for $\Delta E = 25$ MV m^{-1}, the temperature change reaches 2.6 K from 600 K to 1100 K. It is comparable with Li *et al*'s result, which shows an adiabatic temperature change passing

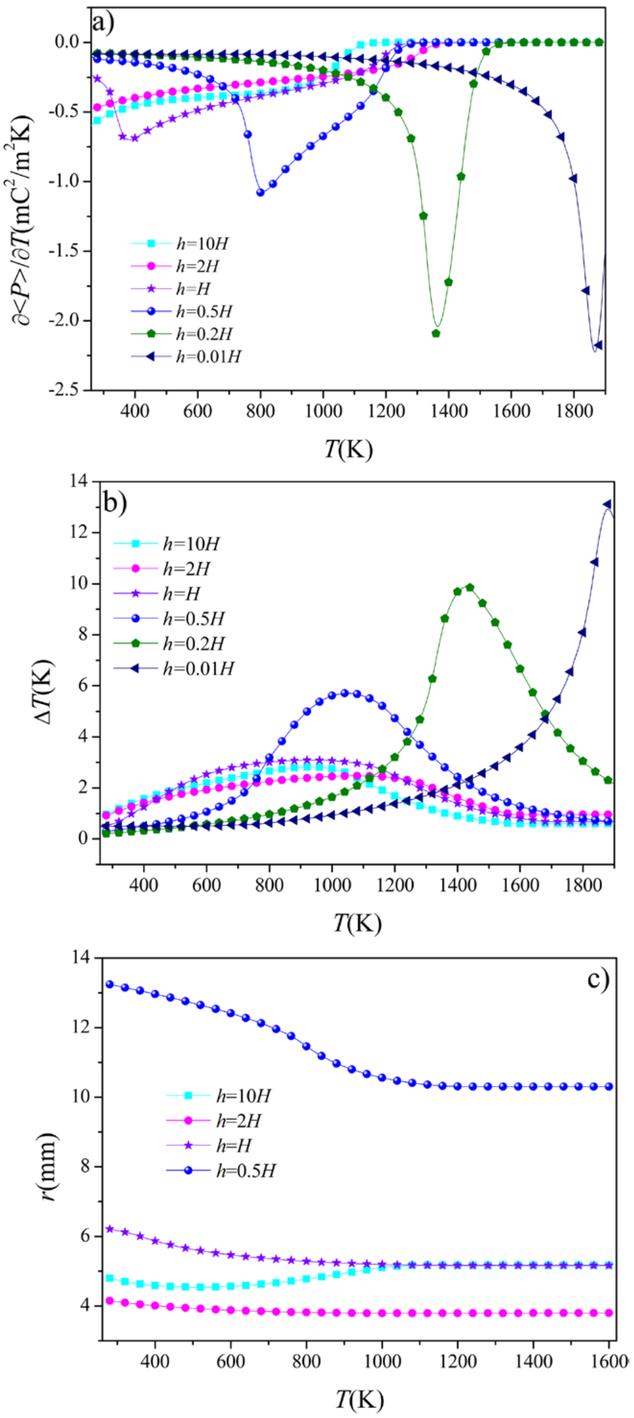

Figure 4. (a) The derivatives of polarization with respect to temperature without external electric field, (b) adiabatic temperature changes under 25 MV m^{-1} electric field shift and (c) radius of curvature without external electric field, as functions of the temperature with various thickness ratios.

over 6 K with a large range between 450 K and 750 K under 30 MV m^{-1} electric field shift by tuning the misfit strain of $PbTiO_3$ thin film [23]. This is almost twice the width of the platform that can be achieved because of the bending effect. In addition, it can be found that, with increased electric field variation, the maximal value of ΔT enhances and shifts progressively to a higher temperature while the width of platform reduces. When ΔE continues increasing to 75 MV m^{-1},

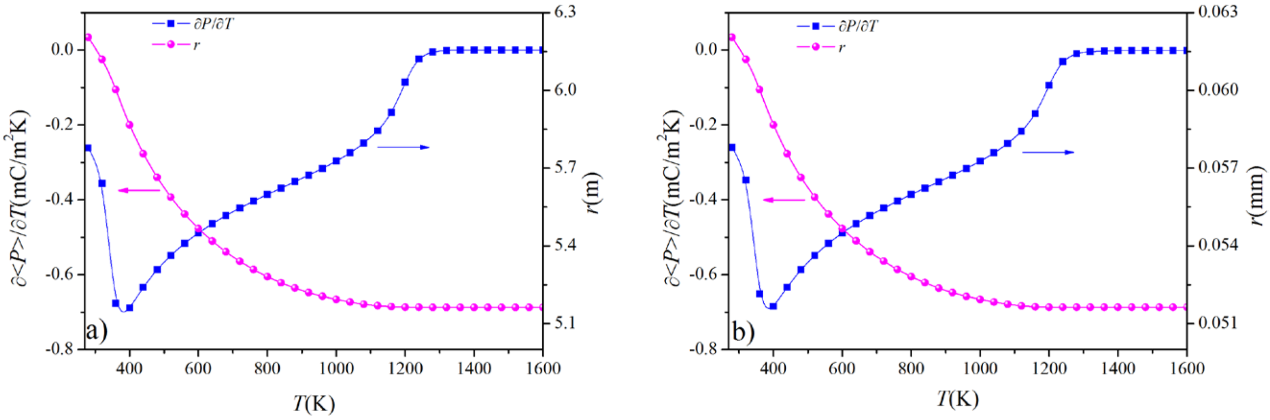

Figure 5. The derivative of polarization with respect to temperature and the radius of curvature with zero applied electric field for (a) $H = h = 0.1$ m and (b) $H = h = 1$ μm.

compared with the result of $LiNbO_3$ which exhibits a shape peak [44], although a hill with the peak value of 8.9 K is formed at 1180 K rather than a platform, ΔT passes over 8 K from 900 K to 1300 K. This phenomenon potentially offers great benefits, and it is reasonable to believe that the platform of adiabatic temperature of bending model can be used for wide temperature refrigeration.

As is commonly known, a material always shows a high EC effect at the phase transition where a significant variation in polarization occurs [8, 45–47]. In order to clarify the origin of the platform, the polarizations as functions of the temperature under various applied electric field are shown in figure 3(a). $<P>$ gradually decreases to zero at 1280 K without the electric field, which represents a significant difference compared with the FE thin film [48]. With increased external electric field, the polarizations represent a lower rate of descent. According to figure 3(a), the derivatives of polarization with respect to temperature applied dynamic external electric field are plotted in figure 3(b). In zero applied electric field, $\partial P/\partial T$ sharply decreases to -0.7mC m^{-2}K^{-1} at 380 K and slowly grows to zero at 1280 K. This result represents a significant difference from the non-bending thin film of which the curve shows an abrupt drop at the phase transition temperature [23]. As for high strength of external electric fields, the peak shifts to right and the curve becomes smoother. Figure 3(c) exhibits the distributions of polarization along z-direction at various temperatures with zero electric field where horizontal axis represents the number of the layer of bending film. It reveals that the polarization decreases along z-direction and the polarization of the last layer from 0.32 C m^{-2} at 300 K tends to zero at 380 K. With $T = 420$ K, the polarization of the last few layers disappear. Thereafter, an increasing number of layers obtain zero-polarization until the PE phase reaches 1280 K. This proves that the phase transition, instead of a shape drop mode converts to a continuous process, starting at 380 K and ending at 1280 K under the bending effect, results in the platform of adiabatic temperature changes.

In order to study the effect of relative thicknesses of FE and PE layers on the adiabatic temperature, we concentrate on the term $\partial P/\partial T$ withdrawing of electric field which according to the equation (12), plays an important role with respect to the EC effect. Figure 4(a) shows the derivatives of polarization with respect to temperature without external electric field versus different thickness ratios in case of $h = 0.1$ mm. For the no-bending condition of $h = 0.01H$ where $h \ll H$, the curve of derivatives represents a sudden decrease to -2.3mC m^{-2}K at 1860 K which is congruent with the classical thin film. When $h = 0.5$ H, the sudden jump disappears. Firstly, $\partial P/\partial T$ decreases quickly to -1.23 mC m^{-2}K^{-1} at 620 K then grows gently to zero at 1290 K. As the thickness ratio increases, the peak location moves to lower temperature with a smaller absolute peak value and the rising process becomes slower. We should note that the critical thickness ratio is $h = 2$ H for which the peak is found at the lowest temperature $T = 160$ K and the value returns to zero at 1340 K. If we continue to augment the relative thicknesses as $h = 10$ H, the peak is located at 200 K with a larger absolute peak value and a narrower range of climbing behavior than that of $h = 2H$. The corresponding temperature changes under 25 MV m^{-1} electric field variation is shown in figure 4(b). As expected, the model of $h = 0.01H$ exhibits an abrupt enhancement of the adiabatic temperature change up to 13.4 K at 1920 K and ΔT in case of $h = 0.5$ H passing over 5.4 K becomes a small platform from 980 K to 1140 K. With increased relative thicknesses before the critical thickness ratio, the coordinate where the largest EC effect occurs shifts to a lower temperature accompanied with expanding of the working range at expense of decreases of ΔT value. Moreover, ΔT of the critical thickness ratio reveals the largest platform from 540 K to 1380 K with the temperature change over 1.7 K. After that, continuously increasing the relative thicknesses has a reverse response of the EC effect. This phenomenon can be explained by the radius of curvature of bilayer system. Based on the equation (5), the radius of curvature r in zero applied electric field is calculated and shown in figure 4(c) with the thickness ratio $h = 0.5H$, $h = H$, $h = 2H$ and $h = 10H$, respectively. Before the critical thickness ratio, the curve of r gradually decreases to a stable value along increased temperatures and the value for every fixed temperature decreases with the augmentation of the thickness ratio. Conversely, compared with the case of $h = 2H$, the value of r with $h = 10H$ is greater for each fixed temperature and the curve of radius decreases until 500 K and then rises to a stable value caused by the competition between the uniform strain c and the term of polarization expressed in equation (5). This demonstrates that a stronger bending response tuned by the thickness ratio will lead to a wider range of temperature changes located at the lower temperature with a smaller value of ΔT.

Finally, we have investigated the influence of the thickness order on the EC effect. According to the previous results, here the radius of curvature and $\partial P/\partial T$ are plotted in figures 5(a) and (b) with $h = H = 0.1$ m and $h = H = 1$ μm respectively. These curves of $\partial P/\partial T$ maintain the same regulation with the result of $h = H = 0.1$ mm shown in figure 4(a). On the other hand, at each temperature, r has the identical tendency and dimensionless values. Therefore, the thickness order doesn't affect the adiabatic temperature change.

Overall, the bending effect, which can induce the strain gradient distribution along z-direction with zero applied electric field, leads to a platform of the large temperature change. The width of the platform, the location of the maximal ΔT and the value of temperature changes which are independent of the thickness order can be adjusted by tuning the relative thicknesses of bilayer.

4. Conclusion

In summary, a FE/PE bilayer system entailing consideration of the bending influence was constructed for investigating the EC effect. The system is set up such that the bending behavior independent of two layers' thickness orders can drive a continuous process of phase transition from FE to PE which characterizes the glass-like transition. Furthermore, the bending effect leads to a platform of the adiabatic temperature change. The width of the platform extends with the decrease of the adiabatic temperature change and the location of the platform shifts to low temperature along the increase of the thickness ratio before the critical value then have the reverse behavior when the relative thickness of system exceed it. This work indicates a possibility of the solid refrigeration application adopting the bending bilayer with a wide range of working window located at low temperature by choosing the appropriate thickness ratio.

Acknowledgments

This project was supported by the NSFC (Nos. 11372361, 11302268, 11232015, 11472321, 1157255), and the Fundamental Research Funds for the Central Universities and the Doctoral Program of Higher Education of China (20120171130003).

References

[1] Kobeko P and Kurchatov I 1930 *Z. Phys.* **66** 192–205
[2] Gu H and Qian X S and Ye H J 2014 *Appl. Phys. Lett.* **99** 162905
[3] Correia T M, Kar-Narayan S, Young J S, Scott J F, Mathur N D, Whatmore R W and Zhang Q 2011 *J. Phys. D: Appl. Phys.* **44** 165407
[4] Li X, Qian X, Lu S G, Cheng J, Fang Z and Zhang Q M 2011 *Appl. Phys. Lett.* **99** 052907
[5] Lee S M and Cahill D G 1997 *J. Appl. Phys.* **81** 2590
[6] Mischenko A S, Zhang Q and Scott J F 2006 *Science* **311** 1270–1
[7] Liu Y, Infante I C and Lou X 2014 *Adv. Mater.* **26** 6132–7
[8] Melvin M V 2013 *J. Phys. D: Appl. Phys.* **46** 345304
[9] Kar-Narayan S and Mathur N D 2010 *J. Phys. D: Appl. Phys.* **43** 032002
[10] De D L and Richet P 1996 *Phys. Rev.* B **53** 3013–22
[11] Moya X, Stern-Taulats E, Crossley S, Gonzalez-Alonso D, Kar-Narayan S, Planes A, Manosa L and Mathur N D 2013 *Adv. Mater.* **25** 1360–5
[12] Wu H H, Zhu J M and Zhang T Y 2015 *Nano Energy* **16** 419–27
[13] Moya X, Kar-Narayan S and Mathur N D 2014 *Nat. Mater.* **13** 439–50
[14] Bai Y, Han X, Zheng X C and Qiao L J 2013 *Sci. Rep.* **3** 2895
[15] Wu H H, Zhu J M, Zhang T Y 2015 *Phys. Chem. Chem. Phys.* **17** 23897–908
[16] Qiu J H and Jiang Q 2013 *J. Appl. Phys.* **523** 034119
[17] Murthy J K and Venimadhav A 2014 *J. Phys. D: Appl. Phys.* **47** 445002
[18] Akcay G and Rossetti S P 2008 *J. Appl. Phys.* **103** 024104
[19] Ma D C, Lin S P, Chen W J, Zheng Y and Wang B. 2014 *AIP Adv.* **4** 107144
[20] Lee J Y, Soh A K, Chen H T and Hong L 2015 *J. Mater. Sci.* **50** 1382–93
[21] Karthik J, Agar J C, Damodaran A R and Martin L W 2012 *Phys. Rev. Lett.* **109** 257602
[22] Fei F, Yang B and Zhang S T 2013 *Appl. Phys. Lett.* **103** 182906
[23] Li B, Zhang X and Wang J B 2014 *Mech. Res. Commun.* **55** 40–4
[24] Morrison F D 2003 *Rev. Adv. Mater. Sci.* **4** 114–22
[25] Morrison F D, Ramsay L and Scott J F 2003 *J. Phys.: Condens. Matter* **15** 527–32
[26] Liu M and Wang J 2015 *Sci. Rep.* **5** 7728
[27] Hernandez-Sanchez B A, Chang K S and Scancella M T 2005 *Chem. Mater.* **17** 5909–19
[28] Morozovska A N and Glinchuk M D 2007 *Phys. Rev.* B **76** 014102
[29] Hong J W and Fang D N 2008 *Appl. Phys. Lett.* **92** 012906
[30] Bhattacharya K and James R D 1999 *J. Mech. Phys. Solids* **47** 531–76
[31] Pertsev N, Zembilgotov A G and Tagantsev A K 1998 *Phys. Rev. Lett.* **80** 236–42
[32] Qiu J H and Jiang Q 2009 *Solid State Commun.* **149** 1549–52
[33] Qiu J H and Ding J N 2013 *Commun. Theor. Phys.* **59** 117–20
[34] Kim J, You H, Ducharme S and Adenwalla S 2007 *J. Phys.: Condens. Matter* **19** 086206
[35] Wu H H, Zhu J M and Zhang T Y 2015 *Rsc. Adv.* **5** 37476–84
[36] Rosse B C 1908 *Nature* **78** 366–7
[37] Wang B and Woo C H 2004 *Acta Mater.* **52** 5639–44
[38] Wang B and Woo C H 2005 *J. Appl. Phys.* **97** 084109
[39] Wang B and Woo C H 2006 *J. Appl. Phys.* **100** 044114
[40] Li Y L, Cross L E and Chen L Q 2005 *J. Appl. Phys.* **98** 064101
[41] Zheng Y, Wang B and Woo C H 2008 *Acta Mater.* **56** 479–88
[42] Wang B and Woo C H 2006 *Appl. Phys. Lett.* **89** 083115
[43] Rabe K M and Ahn C H 2007 *Springer Tr. Mod. Phys.* **86** 203–34
[44] Rose M C and Cohen R E 2012 *Phys. Rev. Lett.* **109** 3368–75
[45] Valant M, Dunne L J, Manos G and Perantie J 2010 *Phys. Rev.* B **81** 214110
[46] Pirc R, Kutnjak Z, Blinc R and Zhang Q M 2011 *J. Appl. Phys.* **110** 074113
[47] Novak N, Pirc R and Kutnjak Z 2013 *Europhys. Lett.* **102** 17003
[48] Liu Y, Peng X P, Lou X J and Zhou H 2012 *Appl. Phys. Lett.* **100** 192902